Acta Cryst E CRYSTALLOGRAPHIC COMMUNICATIONS

ISSN 2056-9890

Crystal structures of the hexafluoridophosphate salts of the isomeric 2-, 3- and 4-cyano-1-methylpyridinium cations and determination of solid-state interaction energies

Joel T. Mague,[a]* Erin Larrabee,[b] David Olivier,[b] Francesca Vaccaro,[b] Kevin E. Riley[c] and Lynn V. Koplitz[b]

[a]Department of Chemistry, Tulane University, New Orleans, LA 70118, USA, [b]Department of Chemistry, Loyola University, New Orleans, LA 70118, USA, and [c]Department of Chemistry, Xavier University of Louisiana, New Orleans, LA 70125, USA. *Correspondence e-mail: joelt@tulane.edu

Received 8 June 2018
Accepted 1 August 2018

Edited by W. T. A. Harrison, University of Aberdeen, Scotland

Keywords: crystal structure; hexafluoridophosphate; cyanopyridinium salts; hydrogen bonds; DFT calculations.

CCDC references: 1859710; 1859709; 1859708

Supporting information: this article has supporting information at journals.iucr.org/e

The synthesis and crystal structures of the isomeric molecular salts 2-, 3- and 4-cyano-1-methylpyridinium hexafluoridophosphate, $C_7H_7N_2^+\cdot PF_6^-$, are reported. In 2-cyano-1-methylpyridinium hexafluoridophosphate, C—H···F hydrogen bonds form chains extending along the *c*-axis direction, which are associated through C—H···F hydrogen bonds and P—F···π(ring) interactions into stepped layers. For 3-cyano-1-methylpyridinium hexafluoridophosphate, corrugated sheets parallel to [001] are generated by C—H···F hydrogen bonds and P—F···π(ring) interactions. The sheets are weakly associated by a weak interaction of the cyano group with the six-membered ring of the cation. In 4-cyano-1-methylpyridinium hexafluoridophosphate, C—H···F hydrogen bonds form a more open three-dimensional network in which stacks of cations and of anions are aligned with the *b*-axis direction. Dispersion-corrected density functional theory (DFT-D) calculations were carried out in order to elucidate some of the energetic aspects of the solid-state structures. The results indicate that the distribution of charge within a molecular ionic cation can play a large role in determining the strength of a cation–anion interaction within a crystal structure. Crystals of 2-cyano-1-methylpyridinium hexafluoridophosphate are twinned by a 180° rotation about the *c** axis. The anion in 3-cyano-1-methylpyridinium hexafluoridophosphate is rotationally disordered by 38.2 (1)° in an 0.848 (3):0.152 (3) ratio.

1. Chemical context

Our interest in the structural features of salts of the cyano-1-methylpyridinium cations (CMP) was generated by the significantly different melting behaviors of 3-CMP chloride and iodide (Koplitz *et al.*, 2003). This was attributed to a greater amount of C—H···N and C—H···*X* (*X* = Cl^-, I^-) hydrogen bonding in the former, in part because all ions lie on mirror planes in the chloride salt while the cation planes are not parallel in the iodide. As a result, it was estimated that the stabilization is at least 1.9 kcal mol^{-1} more in the chloride than in the iodide. At that time, relatively few crystal structures of CMP salts had been published so in order to investigate the packing and non-covalent interactions for these cations in the solid state, structures of salts of the 2-, 3- and 4-CMP^+ cations with a variety of anions including Br^- (Kammer *et al.*, 2012*b*; Mague *et al.*, 2005; Nguyen *et al.*, 2015*b*), I_3^- (Nguyen *et al.*, 2016), I^- (Kammer *et al.*, 2012*a*, 2013), ClO_4^- (Nguyen *et al.*, 2014; Nguyen *et al.*, 2015*a*; McCormick *et al.*, 2014), NO_3^-

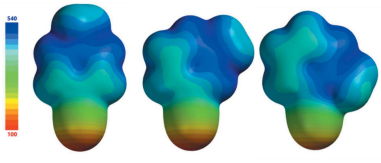

(McCormick *et al.*, 2013; Koplitz *et al.*, 2012) and BF_4^- (Vaccaro *et al.*, 2015) were determined. In addition to structures with parallel sheets as for 3-CMP chloride, ones with interpentrating layers, wrinkled sheets and three-dimensional networks are found. We report here on the hexafluoridophosphate salts of all three cations. More broadly, a better understanding of the manifestations of non-covalent interactions in crystalline organic salts will lead to improved predictions for useful substances in a variety of fields, including materials engineering and targeted drug design. Mapping the crystal structure space for heterocyclic cations in a variety of salts is a very important early step in this overall context.

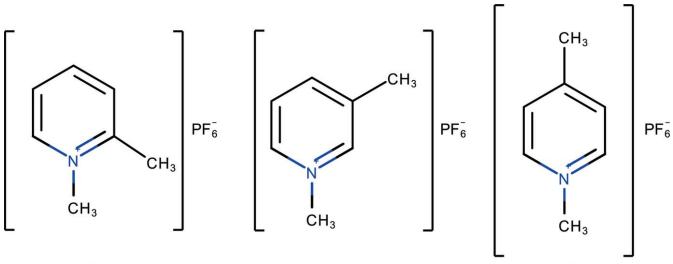

2. Structural commentary

The molecular structures of **1**–**3** are unexceptional in that all three feature essentially planar cations and octahedral anions (Figs. 1, 2 and 3, respectively). The interest lies in their differing solid-state structures and interionic interactions. First, **1** crystallizes in the centrosymmetric space group $P2_1/n$ while **2** and **3** are in the non-centrosymmetric space group $P2_12_12_1$. Second, the number of interionic interactions per asymmetric unit is six in **1**, five in **2** and four in **3**. With no mirror planes present, layer structures are not possible and the cation planes are canted with respect to [100] by ±63.19 (9)° in **1**, ±62.29 (8)° in **2** and ±31.41 (8)° in **3**. In **2** there is a close approach of the cyano group to the six-membered ring of the cation at $x-\frac{1}{2}, -y+\frac{1}{2}, -z+1$ with an N2···centroid distance of 3.322 (4) Å and a C7—N2···centroid angle of 114.4 (3)°.

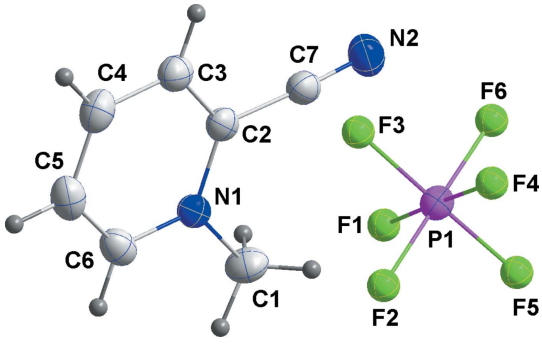

Figure 1
Perspective view of **1** with labeling scheme and 50% probability ellipsoids.

Table 1
Hydrogen-bond geometry (Å, °) for **1**.

D—H···A	D—H	H···A	D···A	D—H···A
C1—H1A···F4^{i}	0.98	2.40	3.161 (3)	134
C1—H1B···F6^{ii}	0.98	2.40	3.307 (3)	154
C4—H4···F6^{iii}	0.95	2.41	3.319 (3)	160
C5—H5···F5^{iv}	0.95	2.51	3.409 (3)	158

Symmetry codes: (i) $-x+\frac{1}{2}, y+\frac{1}{2}, -z+\frac{3}{2}$; (ii) $x+\frac{1}{2}, -y+\frac{3}{2}, z+\frac{1}{2}$; (iii) $x+\frac{1}{2}, -y+\frac{3}{2}, z-\frac{1}{2}$; (iv) $-x+\frac{3}{2}, y+\frac{1}{2}, -z+\frac{3}{2}$.

3. Supramolecular features

In **1**, one cation and one anion are associated through C4—H4···F6 and C5—H5···F5 hydrogen bonds (Table 1) and these units are linked by C1—H1B···F6 hydrogen bonds, forming chains extending along the *c*-axis direction. Pairs of chains are joined by C1—H1A···F4 hydrogen bonds and interactions of F5 and F6 with the six-membered rings at $-x+\frac{1}{2}, y-\frac{1}{2}, -z+\frac{3}{2}$ [F5···centroid = 3.4794 (17) Å, P1—F5···centroid = 105.65 (6)°, F6···centroid = 3.3569 (19) Å, P1—F6···centroid = 110.59 (8)°] of the cations (Table 1 and Fig. 4). The resulting double chains are further joined into stepped layers by C5—H5···F5 hydrogen bonds (Fig. 5).

For **2**, C1—H1B···F4, C2—H2···F6 and C6—H6···F6 hydrogen bonds (Table 2) form zigzag chains (Fig. 6), which

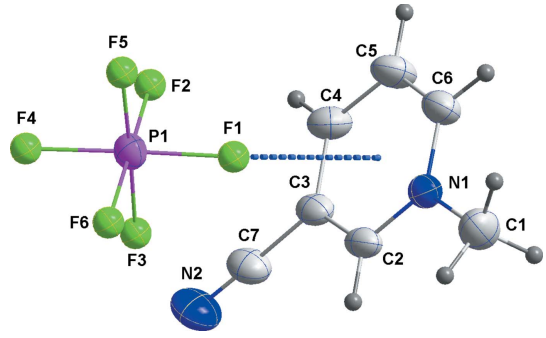

Figure 2
Perspective view of **2** with labeling scheme and 50% probability ellipsoids. Only the major orientation of the disordered anion is shown. The cation–anion interaction is indicated by a dashed line.

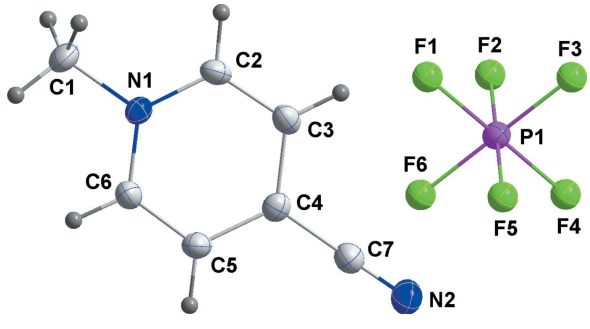

Figure 3
Perspective view of **3** with labeling scheme and 50% probability ellipsoids.

Table 2
Hydrogen-bond geometry (Å, °) for **2**.

D—H···A	D—H	H···A	D···A	D—H···A
C1—H1B···F4^{i}	0.98	2.28	3.225 (5)	161
C2—H2···F6^{i}	0.95	2.34	3.253 (4)	160
C6—H6···F6^{ii}	0.95	2.53	3.389 (5)	150

Symmetry codes: (i) $-x+1, y-\frac{1}{2}, -z+\frac{3}{2}$; (ii) $x+1, y, z$.

Table 3
Hydrogen-bond geometry (Å, °) for **3**.

D—H···A	D—H	H···A	D···A	D—H···A
C5—H5···F5^{i}	0.95	2.37	3.247 (2)	153
C3—H3···F3^{ii}	0.95	2.46	3.106 (2)	126
C1—H1C···F1^{iii}	0.98	2.51	3.208 (3)	128

Symmetry codes: (i) $-x+\frac{1}{2}, -y, z-\frac{1}{2}$; (ii) $-x+1, y+\frac{1}{2}, -z+\frac{3}{2}$; (iii) $-x+\frac{1}{2}, -y+1, z-\frac{1}{2}$.

are joined by the close interaction of F1 with the six-membered rings of the cations [F1···centroid = 3.186 (3) Å, P1—F1···centroid = 123.67 (12)°, forming corrugated sheets parallel to [001]. These sheets are associated through the weak interaction of the cyano group with the six-membered ring of the cation mentioned in the preceding section (Fig. 7).

In **3**, a relatively open, three-dimensional network structure in which stacks of cations and of anions are aligned with the *b*-axis direction is generated by C1—H1C···F1, C3—H3···F3 and C5—H5···F5 hydrogen bonds (Table 3 and Figs. 8 and 9).

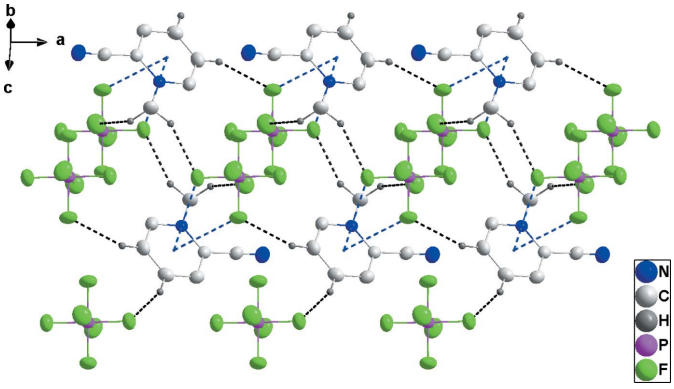

Figure 4
Side view of two cation and anion columns in **1** projected onto (021). C—H···F hydrogen bonds are shown as black dashed lines and P—F···π(ring) interactions by blue dashed lines.

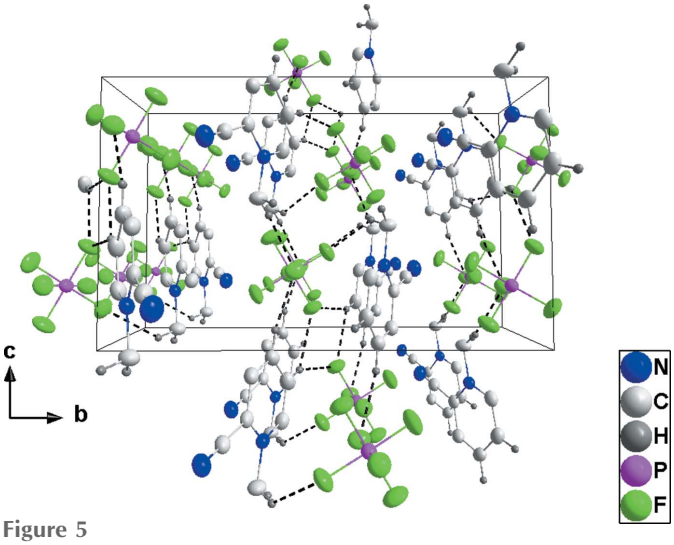

Figure 5
Packing of **1** viewed along the *a*-axis direction with C—H···F hydrogen bonds shown as dashed lines.

4. DFT studies

Dispersion-corrected density functional theory (DFT-D) calculations were carried out in order to elucidate some of the energetic aspects of the CMP-PF_6 structures. Calculations

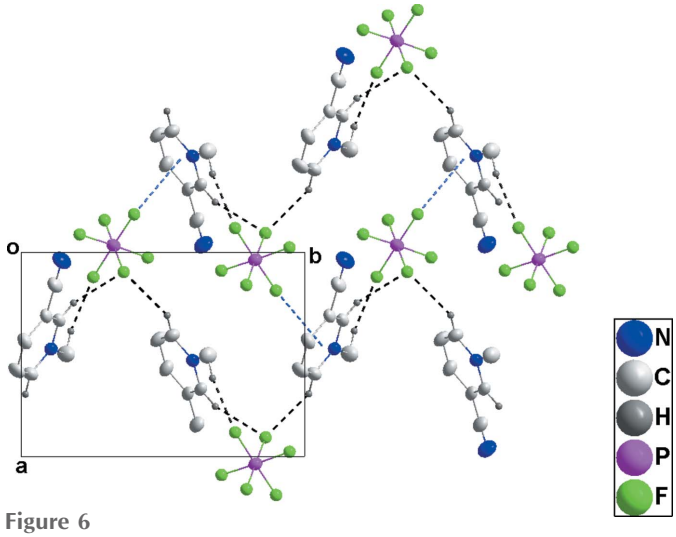

Figure 6
View of two adjacent cation–anion chains in **2** along the *c*-axis direction with C—H···F hydrogen bonds shown by black dashed lines.

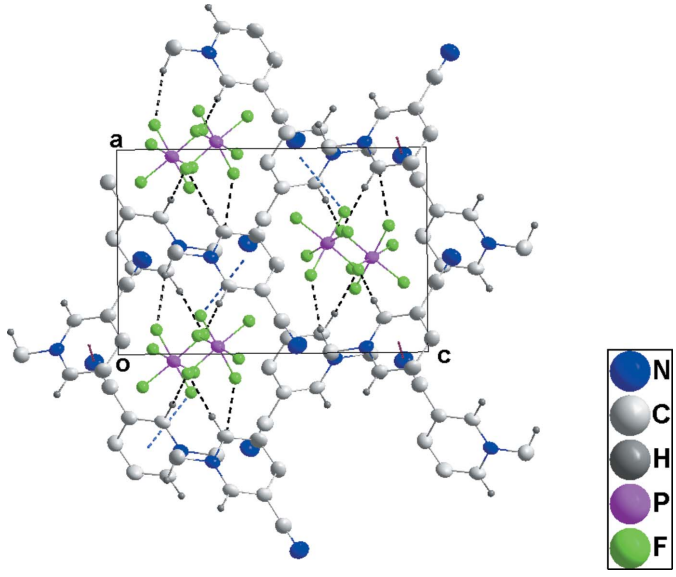

Figure 7
Packing of **2** viewed along the *b*-axis direction. C—H···F hydrogen bonds and P—F···π(ring) and C≡N···π(ring) interactions are shown, respectively, by black, blue and purple dashed lines.

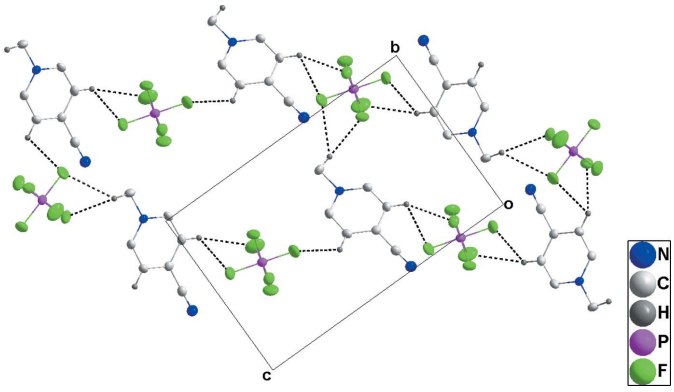

Figure 8
View of two adjacent cation–anion chains in **3** along the *a*-axis direction with C—H···F hydrogen bonds shown by black dashed lines.

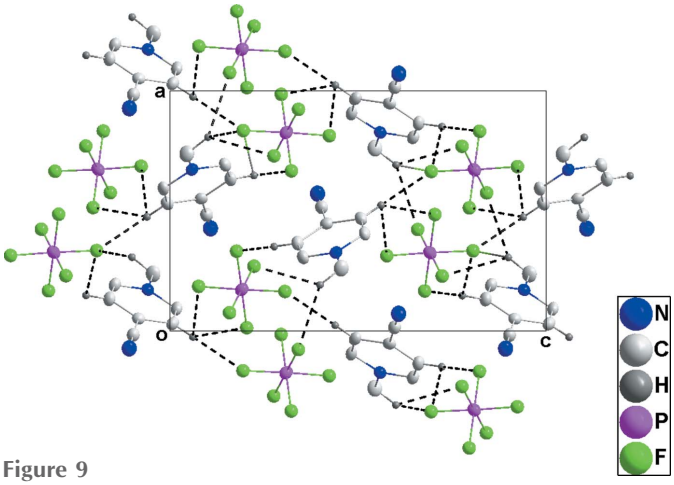

Figure 9
Packing of **3** viewed along the *b*-axis direction. C—H···F hydrogen bonds are shown by black dashed lines.

were carried out at the ωB97X-D/def2-TZVP level of theory (Jurečka *et al.*, 2007; Chai & Head-Gordon, 2008; Grimme, 2006; Schröder *et al.*, 2017). Here, all computations are carried out using the SMD (solvation model based on density) model in order to approximate the effect of the crystal environment (Marenich *et al.*, 2009). The dielectric constant of the CMP-PF_6 crystals is currently unknown, so a dielectric constant of 4.0 was chosen as a generic value (as has been done in previous studies; Nguyen *et al.*, 2016). Although the interactions under consideration are between molecular cations and anions, and complex stabilization is therefore attributable mainly to electrostatic forces, it is important that all attractive and repulsive forces (induction, dispersion, exchange) be modeled as well as possible. As DFT is known to describe dispersion interactions very poorly, here we have used a model incorporating an empirical dispersion term (-D2) in order to account for this shortcoming (Grimme, 2006). Dispersion plays a substantial role in stabilizing all non-covalent complexes (Riley *et al.*, 2010; Johnson *et al.*, 2010) and is known to be especially important in larger aliphatic and aromatic molecules (Sedlak *et al.*, 2013). It has been shown that the parameterizations of empirical dispersion terms, which are generally established from gas-phase benchmark

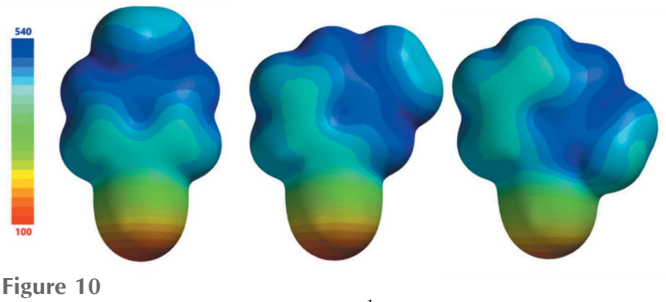

Figure 10
Electrostatic potential maps (kcal mol^{-1}) for the 4-CMP^+ (left), 3-CMP^+ (center) and 2-CMP^+ (right) cations. Note the large range of 440 kcal mol^{-1}. The strong electron-withdrawing ability of the cyano group results in a significantly less positive partial charge for that part of the molecular ion.

data, remain essentially unchanged when implicit solvent models, such as SMD, are used (Riley *et al.*, 2007).

Electrostatic potentials for the three CMP molecular cations (Fig. 10) and the PF_6^- anion (Fig. 11) were obtained at the B3LYP/6-311+G** level of theory. It has been shown that the quality of an electrostatic potential does not strongly depend on the level of theory (DFT or HF) or on the particular basis set used, so long as the basis set is sufficiently large (at least 6-31G*; Riley *et al.*, 2016). The most interesting aspect of these electrostatic potentials concerns the molecular cations, for which there are seen to be large shifts in charge density from one part of the molecular ion to another, with the most positive regions having potential values of 140 (**1**), 109 (**2**), and 108 (**3**) kcal mol^{-1} and the least positive regions having values of 529 (**1**), 533 (**2**), and 531 (**3**) kcal mol^{-1}. This large shift in charge from one region to another is principally attributable to the high electron-withdrawing capacity of the cyano group, resulting in a less positive partial charge in that region of the molecular ion. For all three molecular cations, the most positively charged regions are those neighboring the CMP methyl groups (*i.e.* the H atoms that are *ortho*- to the methyl groups), with the exception of the region located between the methyl and cyano groups in **1**. As will be discussed below, the anisotropic distribution of charge throughout these molecular cations has significant effects on the strengths of the interactions (Table 4) between these moieties and the PF_6^- anions.

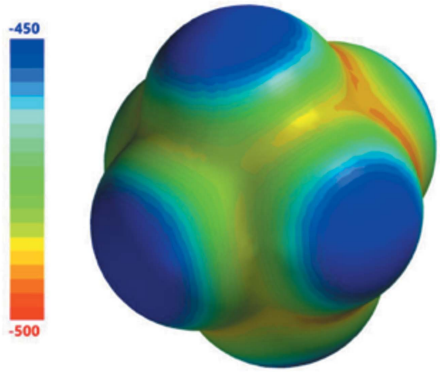

Figure 11
Electrostatic potential map (kcal mol^{-1}) for the hexafluoridophosphate anion. Note the relatively small range of 50 kcal mol^{-1}.

Table 4
Cation–anion interaction energies (kcal mol^{-1}).

Compound **1**		Compound **2**		Compound **3**	
D—H···A	ΔE_{int}	D—H···A	ΔE_{int}	D—H···A	ΔE_{int}
C1—H1A···F4^{i}	−19.0	C1—H1B···F4^{iv}	−16.6	C5—H5···F5^{vi}	−14.2
C1—H1B···F6^{ii}	−15.9	C2—H2···F6^{iv}	−16.6	C3—H3···F3^{vii}	−15.3
C4—H4···F6	−15.7	C6—H6···F6^{v}	−17.8	C1—H1C···F1^{viii}	−16.7
C5—H5···F5^{iii}	−15.9				

Symmetry codes: (i) $-x+\frac{1}{2}, y+\frac{1}{2}, -z+\frac{3}{2}$; (ii) $x+\frac{1}{2}, -y+\frac{3}{2}, z+\frac{1}{2}$; (iii) $-x+\frac{3}{2}, y+\frac{1}{2}, -z+\frac{3}{2}$; (iv) $-x+1, y-\frac{1}{2}, -z+\frac{3}{2}$; (v) $x+1, y, z$; (vi) $-x+\frac{1}{2}, -y, z-\frac{1}{2}$; (vii) $-x+1, y+\frac{1}{2}, -z+\frac{3}{2}$; (viii) $-x+\frac{1}{2}, -y+1, z-\frac{1}{2}$.

The shortest cation–anion contacts within the crystal structure of **1** are shown in Fig. 12. Here it is seen that three of the molecular cations (shown in cyan, pink, and yellow) have aromatic rings that are coplanar with each other and are quasi-coplanar with three fluorine atoms from the PF_6^- anion. In each case, two contacts are made between a cation H atom and one of the quasi-coplanar PF_6^- fluorine atoms, although it should be noted that the longest contact in the interaction involving the pink cation (3.59 Å) is substantially longer than all other contacts (2.40–2.62 Å). Two of the shorter contacts involving aromatic hydrogen atoms (cyan, yellow) and one involving a methyl hydrogen atom (purple). The fourth close contact (green) is a stacking interaction involves a 2-CMP cation located in a plane below PF_6^- (as depicted), with a short C—H···F contact occurring between a methyl H atom and an anion F atom.

Unsurprisingly, among the four cation–anion pairs given in Fig. 12, the stacking contact (green) represents the strongest interaction, with a binding energy of −19.0 kcal mol^{-1}. The strength of this interaction is mainly due to the large area of contact between cation and ion, with three F atoms within a distance of 3.4 Å from the cation. Without knowledge of the electronic density distribution, as reflected in the electrostatic potential, it might be assumed that the strongest interaction among the PF_6^- contacts with the three coplanar molecular cations would be that involving the yellow cation, which exhibits the shortest contact distances with the PF_6^- anion. Thus, it is somewhat surprising that this interaction is actually

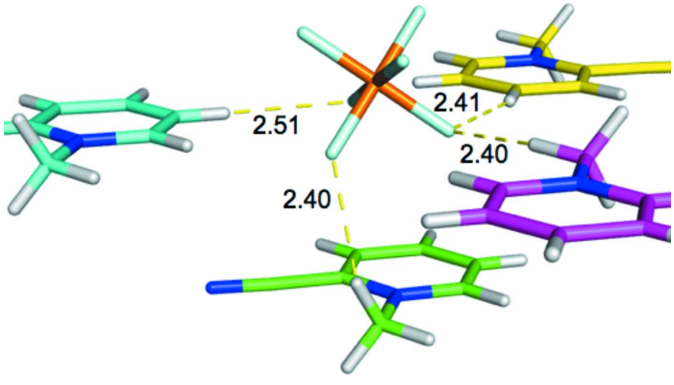

Figure 12
2-CMP$^+$···PF_6^- interactions. BLYP-D3/def2-TZVP/SMD interaction energies (kcal mol^{-1}) for these complexes are: −19.0 (green), −16.9 (cyan), −15.9 (purple), and −15.7 (yellow).

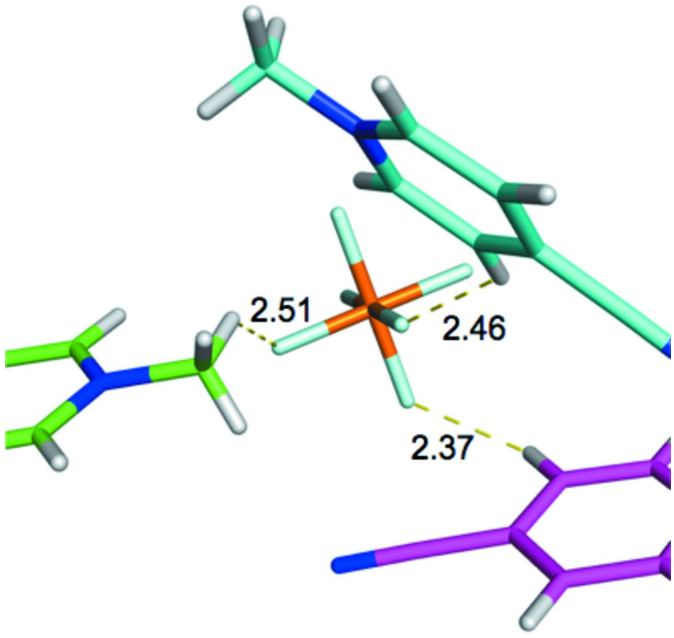

Figure 13
4-CMP$^+$···PF_6^- interactions. BLYP-D3/def2-TZVP/SMD interaction energies (kcal mol^{-1}) for these complexes are: −16.7 (green), −15.3 (cyan), −14.2 (purple).

predicted to be the *weakest* among the coplanar interactions, with an interaction energy of −15.7 kcal mol^{-1}. Surprisingly, even the coplanar interaction with only one short H$^+$···F$^-$ contact (purple) exhibits slightly stronger attraction (−15.9 kcal mol^{-1}), while the strongest interaction (−16.9 kcal mol^{-1}) occurs for the cyan cation, whose contact distances are slightly longer than those of the interaction involving the yellow cation.

The counter-intuitive results described above can be explained by considering the distribution of charge on 2-CMP$^+$, as reflected in the electrostatic potential. The most positive region of the 2-CMP$^+$ cation encompasses the hydrogen neighboring the methyl group and the N—CH_3 bond. Each of the two stronger complexes (cyan, purple) includes a contact between this strongly positive region of the electrostatic potential and a negative F atom. Conversely the shortest contact in the weaker of these complexes (yellow) involves the H atom that is *para*- to the methyl group, the least positively charged of the aromatic hydrogen atoms.

The details of cation charge distribution are again seen to be important in determining interaction strengths within the crystal structure of **3**. In Fig. 13 it is seen that the strongest interaction involves the green 4-CMP$^+$ molecular cation (−16.7 kcal mol^{-1}), whose shortest H$^+$···F$^-$ contact (involving a methyl H atom) is the longest (2.51 Å) among the three interactions considered here. The enhanced strength of this interaction, relative to the other two contacts, can be explained by the orientation of the 4-CMP$^+$ cation relative to the PF_6^- anion. As seen in Fig. 10, the regions neighboring the methyl group on the 4-CMP$^+$ cation are significantly more positive than other regions of the molecular ion. It is this highly positive region that forms contact with the PF_6^- anion,

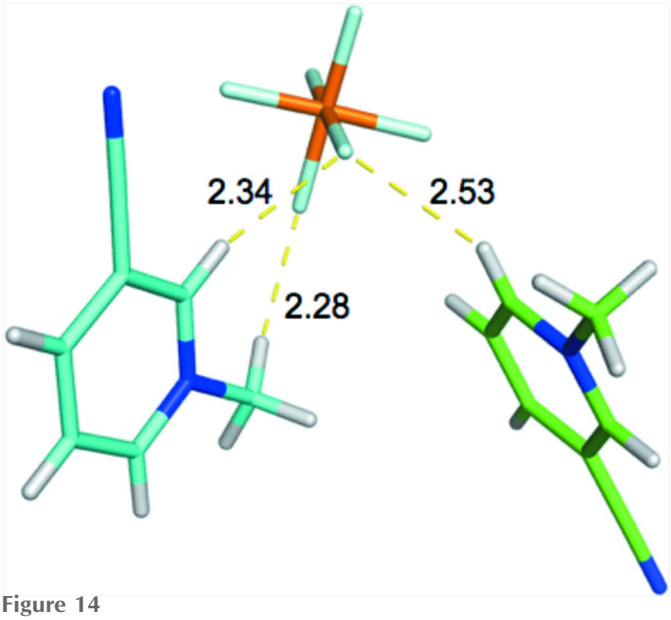

Figure 14
3-CMP$^{+}\cdots PF_6^{-}$ interactions. BLYP-D3/def2-TZVP/SMD interaction energies (kcal mol^{-1}) −17.8 for these complexes are: (green) and −16.6 (cyan).

as shown in Fig. 13. The weakest interaction here involves the pink 4-CMP^{+} cation (−14.2 kcal mol^{-1}), whose closest $H^{+}\cdots F^{-}$ distance (2.37 Å) is the shortest among all contacts considered here. This contact involves a hydrogen atom that neighbors the 4-CMP cyano group, which is located in a region whose positive charge is relatively low.

The ordering of the interaction strengths for the two complexes involving the 3-CMP^{+} cations, shown in Fig. 14, are also counter-intuitive. The interaction with the shorter $H^{+}\cdots F^{-}$ distances (cyan) represents the weaker of the two interactions. The stronger of the two interactions (green) involves the aromatic H atom that is *para*- to the cyano group, located on the most positive region of the cation. The proximity of this positive region to the anion is likely responsible for the stronger binding of this cation.

Results presented here indicate that the distribution of charge within a molecular ionic cation can play a large role in determining the strength of a cation–anion interaction within a crystal structure. It is presumed that careful inspection of electrostatic potentials becomes more important as the size of a cation increases and as strong electron-withdrawing groups, such as cyano groups, are introduced. Although not investigated here, similar trends are likely observed for larger molecular anions.

5. Database survey

In addition to those compounds cited in the *Chemical context* section, there are 14 other structures in the CSD (Version 5.39; Groom *et al.*, 2016) containing cyano-1-methyl pyridinium cations. Of these, ten contain the 4-CMP cation and the other four the 3-CMP cation. Both 3- and 4-CMP[$N(SO_2CF_3)_2$] are described with the former having a layer structure formed from cation chains involving C—H···N interactions between a ring hydrogen atom and the cyano group, which are bound to anion chains by C_{ring}—H···O and C_{methyl}—H···N hydrogen bonds. The layers have the trifluoromethyl groups protruding from one face and the *para* ring hydrogens from the other. The latter has a three-dimensional network structure in which only the ring hydrogen atoms form C—H···O hydrogen bonds, leading to channels along the *a*-axis direction with the cyano, methyl and trifluoromethyl groups forming the inner edges (Hardacre *et al.*, 2008). The co-crystal of 4-CMP[$N(SO_2CF_3)_2$] with 1-methylnapthalene has corrugated layers of alternating cations and anions with trifluromethyl groups protruding from both faces interspersed with layers of 1-methylnapthalene (Hardacre *et al.*, 2010). In 4-CMP[CH_3OSO_3], C—H···O hydrogen bonds involving both aromatic and aliphatic H atoms form cation–anion chains along the *c*-axis direction, which are joined into double layers having the anion methyl groups protruding from both faces by C_{methyl}—H···O hydrogen bonds (Hardacre *et al.*, 2008). A different structure is found in 4-CMP[$Co(CO)_4$] where pairwise C_{ring}—H···N interactions form dimers that are expanded into cross-linked zigzag chains by C_{ring}—H···O hydrogen bonds with the anions (Bockman & Kochi, 1989). Cross-linked, zigzag chains are also found in 4-CMP[ZnI_4], but here the chains are only cations and are formed by C_{methyl}—H···N interactions. The anions serve to cross-link them through C_{ring}—H···I and C_{methyl}—H···I interactions (Glavcheva *et al.*, 2004). Another example of a layer structure is in [4-CMP]$_2$[$Cu[S_2C_2(CN)_2]_2$] where alternating cation–anion chains are formed with half of the cations and the anions through C_{ring}—H···N hydrogen bonds. The remaining cations use C_{ring}—H···N hydrogen bonds to both cations and anions in the chains to form a three-dimensional network (Wang *et al.*, 2012).

The remaining structures feature large anions, but this does not necessarily isolate the cations from each other. In 4-CMP[{HB(3,5-dimethylpyrazolyl)$_3$}$Mo(CO)_3$], the cations form dimers as in 4-CMP[$Co(CO)_4$] and are associated with the anions through C_{ring}—H···O hydrogen bonds as well as a π–π stacking interaction with one of the pyrazolyl rings (Bockman & Kochi, 1992). An entirely different structure is seen in $\{(4\text{-CMP})_2[Cu_4(\mu_3\text{-I})(\mu\text{-I})_2]\}_n$ where zigzag chains of cations formed by C_{ring}—H···N hydrogen bonds are arranged at right angles to one another between chains of anions and link the latter through C_{methyl}—H···I interactions (Chan *et al.*, 2012). Similar zigzag chains of cations are found in $\{(3\text{-CMP})[Ag_4(\mu_4\text{-I})_2(\mu\text{-I})_2(\mu\text{-I})]\}_n$ but here they are all coplanar in a layer structure where cation and anion layers alternate (Yu *et al.*, 2014). Details of the interionic interactions in $\{(4\text{-CMP})[Ag_2I_3]\}_n$ (Shen *et al.*, 2014) and (3-CMP)BPh_4 (Zhu & Kochi, 1999) are obscured by considerable disorder.

6. Synthesis and crystallization

2-Cyano-1-methylpyridinium hexafluoridophosphate (1)

To a solution of 2.499 g (1.016 mmol) of 2-cyano-1-methyl pyridinium iodide (Kammer *et al.*, 2013) dissolved in 20 ml of deionized water was added 1.87 g (1.221 mmol) of solid

Table 5
Experimental details.

	1	2	3
Crystal data			
Chemical formula	$C_7H_7N_2^+\cdot PF_6^-$	$C_7H_7N_2^+\cdot PF_6^-$	$C_7H_7N_2^+\cdot PF_6^-$
M_r	264.12	264.12	264.12
Crystal system, space group	Monoclinic, $P2_1/n$	Orthorhombic, $P2_12_12_1$	Orthorhombic, $P2_12_12_1$
Temperature (K)	150	150	150
a, b, c (Å)	6.5296 (5), 15.7145 (13), 9.5550 (7)	7.8484 (2), 10.8964 (2), 11.8669 (3)	8.5293 (6), 8.6264 (7), 13.3589 (10)
α, β, γ (°)	90, 93.327 (4), 90	90, 90, 90	90, 90, 90
V (Å^3)	978.78 (13)	1014.85 (4)	982.91 (13)
Z	4	4	4
Radiation type	Cu $K\alpha$	Cu $K\alpha$	Mo $K\alpha$
μ (mm^{-1})	3.21	3.09	0.34
Crystal size (mm)	0.20 × 0.17 × 0.06	0.26 × 0.19 × 0.15	0.26 × 0.19 × 0.13
Data collection			
Diffractometer	Bruker D8 VENTURE PHOTON 100 CMOS	Bruker D8 VENTURE PHOTON 100 CMOS	Bruker *SMART APEX* CCD
Absorption correction	Multi-scan (*TWINABS*; Sheldrick, 2009)	Multi-scan (*SADABS*; Bruker, 2015)	Multi-scan (*SADABS*; Bruker, 2015)
T_{min}, T_{max}	0.57, 0.84	0.59, 0.65	0.89, 0.96
No. of measured, independent and observed [$I > 2\sigma(I)$] reflections	12567, 1895, 1692	15204, 2009, 1970	19081, 2642, 2420
R_{int}	0.040	0.034	0.033
(sin $\theta/\lambda)_{max}$ (Å^{-1})	0.618	0.618	0.686
Refinement			
$R[F^2 > 2\sigma(F^2)]$, $wR(F^2)$, S	0.042, 0.115, 1.07	0.036, 0.095, 1.08	0.031, 0.084, 1.13
No. of reflections	1895	2009	2642
No. of parameters	147	160	146
No. of restraints	0	8	0
H-atom treatment	H-atom parameters constrained	H-atom parameters constrained	H-atom parameters constrained
$\Delta\rho_{max}$, $\Delta\rho_{min}$ (e Å^{-3})	0.31, −0.33	0.35, −0.36	0.31, −0.20
Absolute structure	–	Flack x determined using 800 quotients $[(I^+)-(I^-)]/[(I^+)+(I^-)]$ (Parsons *et al.*, 2013)	Flack x determined using 988 quotients $[(I^+)-(I^-)]/[(I^+)+(I^-)]$ (Parsons *et al.*, 2013)
Absolute structure parameter	–	0.040 (6)	−0.01 (3)

Computer programs: *APEX2* and *SAINT* (Bruker, 2015), *CELL_NOW* (Sheldrick, 2008*b*), *SHELXT* (Sheldrick, 2015*a*), *SHELXL* (Sheldrick, 2015*b*), *DIAMOND* (Brandenburg & Putz, 2012) and *SHELXTL* (Sheldrick, 2008*a*).

potassium hexafluoridophosphate with stirring. The white solid that precipitated was washed with a small quantity of ice-cold, deionized water and recrystallized from deionized water by slow evaporation under a gentle stream of nitrogen. M.p. 379 K.

3-Cyano-1-methylpyridinium hexafluoridophosphate (2)

This was prepared and crystallized in analogous manner to that for **1** using 2.508 g (1.019 mmol) of 3-cyano-1-methylpyridinium iodide and 1.873 g (1.223 mmol) of solid potassium hexafluoridophosphate. M.p. 394 K.

4-Cyano-1-methylpyridinium hexafluoridophosphate (3)

This was prepared and crystallized in analogous manner to that for **1** using 2.491 g (1.012 mmol) of 4-cyano-1-methylpyridinium iodide and 1.873 g (1.223 mmol) of solid potassium hexafluoridophosphate. M.p. 418 K.

7. Refinement details

Crystal data, data collection and structure refinement details are summarized in Table 5. Crystals of **1** are twinned by a 180° rotation about the c^* axis. Trial refinements of this structure with the single-component reflection file extracted from the twinned data set with *TWINABS* (Sheldrick, 2009) and the full 2-component reflection file showed the former to be more satisfactory. The anion in **2** is rotationally disordered by 38.2 (1)° about the F1—P1—F4 axis in an 0.848 (3):0.152 (3) ratio. The two components of the disorder were refined with restraints that their geometries be comparable. H atoms were placed in calculated positions and refined using a riding model: C—H = 0.98 Å with U_{iso}(H) = 1.5U_{eq}(C) for methyl H atoms, C—H = 0.95 Å with U_{iso}(H) = 1.2U_{eq}(C) for all other H atoms.

Funding information

The support of NSF–MRI grant No. 1228232 for the purchase of the diffractometer and Tulane University for support of the Tulane Crystallography Laboratory are gratefully acknowledged. LVK acknowledges generous support from the Earl and Gertrude Vicknair Distinguished Professorship in Chemistry at Loyola University.

References

Bockman, T. M. & Kochi, J. K. (1989). *J. Am. Chem. Soc.* **111**, 4669–4683.
Bockman, T. M. & Kochi, J. K. (1992). *New J. Chem.* **16**, 39–49.
Brandenburg, K. & Putz, H. (2012). *DIAMOND*, Crystal Impact GbR, Bonn, Germany.

Bruker (2015). *APEX2* and *SAINT*. Bruker AXS Inc., Madison, Wisconsin, USA.
Chai, J.-D. & Head-Gordon, M. (2008). *Phys. Chem. Chem. Phys.* **10**, 6615–6620.
Chan, H., Chen, Y., Dai, M., Lu, C.-N., Wang, H.-F., Ren, Z.-G., Huang, Z.-J., Ni, C.-Y. & Lang, J.-P. (2012). *ChemEngComm.* **14**, 466–473.
Glavcheva, Z., Umezawa, H., Okada, S. & Nakanishi, H. (2004). *Mater. Lett.* **58**, 2466–2471.
Grimme, S. (2006). *J. Comput. Chem.* **27**, 1787–1799.
Groom, C. R., Bruno, I. J., Lightfoot, M. P. & Ward, S. C. (2016). *Acta Cryst.* B**72**, 171–179.
Hardacre, C., Holbrey, J. D., Mullan, C. L., Nieuwenhuyzen, M., Reichert, W. M., Seddon, K. R. & Teat, S. J. (2008). *New J. Chem.* **32**, 1953–1967.
Hardacre, C., Holbrey, J. D., Mullan, C. L., Nieuwenhuyzen, M., Youngs, T. G. A., Bowron, D. T. & Teat, S. J. (2010). *Phys. Chem. Chem. Phys.* **12**, 1842–1853.
Johnson, E. R., Keinan, S., Mori-Sánchez, P., Contreras-García, J., Cohen, A. J. & Yang, W. (2010). *J. Am. Chem. Soc.* **132**, 6498–6506.
Jurečka, P., Černý, J., Hobza, P. & Salahub, D. (2007). *J. Comput. Chem.* **28**, 555–569.
Kammer, M. N., Koplitz, L. V. & Mague, J. T. (2012*a*). *Acta Cryst.* E**68**, o2514.
Kammer, M. N., Koplitz, L. V. & Mague, J. T. (2013). *Acta Cryst.* E**69**, o1281.
Kammer, M. N., Mague, J. T. & Koplitz, L. V. (2012*b*). *Acta Cryst.* E**68**, o2409.
Koplitz, L. V., Bay, K. D., DiGiovanni, N. & Mague, J. T. (2003). *J. Chem. Cryst.* **33**, 391–402.
Koplitz, L. V., Mague, J. T., Kammer, M. N., McCormick, C. A., Renfro, H. E. & Vumbaco, D. J. (2012). *Acta Cryst.* E**68**, o1653.
Mague, J. T., Ivie, R. M., Hartsock, R. W., Koplitz, L. V. & Spulak, M. (2005). *Acta Cryst.* E**61**, o851–o853.
Marenich, A. V., Cramer, C. J. & Truhlar, D. G. (2009). *J. Phys. Chem. B*, **113**, 4538–4543.
McCormick, C. A., Nguyen, V. D., Koplitz, L. V. & Mague, J. T. (2014). *Acta Cryst.* E**70**, o811.
McCormick, C. A., Nguyen, V. D., Renfro, H. E., Koplitz, L. V. & Mague, J. T. (2013). *Acta Cryst.* E**69**, o981–o982.
Nguyen, V. D., McCormick, C. A., Koplitz, L. V. & Mague, J. T. (2014). *Acta Cryst.* E**70**, o756–o757.
Nguyen, V. D., McCormick, C. A., Mague, J. T. & Koplitz, L. V. (2015*a*). *Acta Cryst.* E**71**, o852–o853.
Nguyen, V. D., McCormick, C. A., Pascal, R. A., Mague, J. T. & Koplitz, L. V. (2015b). *Acta Cryst.* E**71**, o854–o855.
Nguyen, V. D., McCormick, C. A., Vaccaro, F. A., Riley, K. E., Stephenson, C. J., Mague, J. T. & Koplitz, L. V. (2016). *Polyhedron*, **114**, 428–434.
Parsons, S., Flack, H. D. & Wagner, T. (2013). *Acta Cryst.* B**69**, 249–259.
Riley, K. E., Pitoňák, M., Jurečka, P. & Hobza, P. (2010). *Chem. Rev.* **110**, 5023–5063.
Riley, K. E., Tran, K. A., Lane, P., Murray, J. S. & Politzer, P. (2016). *J. Comput. Sci.* **17**, 273–284.
Riley, K. E., Vondrášek, J. & Hobza, P. (2007). *Phys. Chem. Chem. Phys.* **9**, 5555–5560.
Schröder, H., Hühnert, J. & Schwabe, T. (2017). *J. Chem. Phys.* **146**, 044115.
Sedlak, R., Janowski, T., Pitoňák, M., Řezáč, J., Pulay, P. & Hobza, P. (2013). *J. Chem. Theory Comput.* **9**, 3364–3374.
Sheldrick, G. M. (2008*a*). *Acta Cryst.* A**64**, 112–122.
Sheldrick, G. M. (2008*b*). *CELL_NOW*, University of Göttingen, Göttingen, Germany.
Sheldrick, G. M. (2009). *TWINABS*, University of Göttingen, Göttingen, Germany.
Sheldrick, G. M. (2015*a*). *Acta Cryst.* A**71**, 3–8.
Sheldrick, G. M. (2015*b*). *Acta Cryst.* C**71**, 3–8.
Shen, J., Zhang, C., Yu, T., An, L. & Fu, Y. (2014). *Cryst. Growth Des.* **14**, 6337–6342.
Vaccaro, F. A., Koplitz, L. V. & Mague, J. T. (2015). *Acta Cryst.* E**71**, o697–o698.
Wang, N., Wang, J.-G., Min, A.-J. & Fu, Y.-W. (2012). *Acta Cryst.* E**68**, m164.
Yu, T.-L., An, L., Zhang, L., Shen, J.-J., Fu, Y.-B. & Fu, Y.-L. (2014). *Cryst. Growth Des.* **14**, 3875–3879.
Zhu, D. & Kochi, J. K. (1999). *Organometallics*, **18**, 161–172.

supporting information

Acta Cryst. (2018). E**74**, 1322-1329 [https://doi.org/10.1107/S2056989018011003]

Crystal structures of the hexafluoridophosphate salts of the isomeric 2-, 3- and 4-cyano-1-methylpyridinium cations and determination of solid-state interaction energies

Joel T. Mague, Erin Larrabee, David Olivier, Francesca Vaccaro, Kevin E. Riley and Lynn V. Koplitz

Computing details

For all structures, data collection: *APEX2* (Bruker, 2015); cell refinement: *SAINT* (Bruker, 2015). Data reduction: *SAINT* (Bruker, 2015), *CELL_NOW* (Sheldrick, 2008b) for (1); *SAINT* (Bruker, 2015) for (2), (3). For all structures, program(s) used to solve structure: *SHELXT* (Sheldrick, 2015a); program(s) used to refine structure: *SHELXL* (Sheldrick, 2015b); molecular graphics: *DIAMOND* (Brandenburg & Putz, 2012); software used to prepare material for publication: *SHELXTL* (Sheldrick, 2008a).

2-Cyano-1-methylpyridinium hexafluoridophosphate (1)

Crystal data

$C_7H_7N_2^+\cdot PF_6^-$
M_r = 264.12
Monoclinic, $P2_1/n$
a = 6.5296 (5) Å
b = 15.7145 (13) Å
c = 9.5550 (7) Å
β = 93.327 (4)°
V = 978.78 (13) Å^3
Z = 4
$F(000)$ = 528
D_x = 1.792 Mg m^{-3}
Cu $K\alpha$ radiation, λ = 1.54178 Å
Cell parameters from 2191 reflections
θ = 7.3–71.9°
μ = 3.21 mm^{-1}
T = 150 K
Plate, colourless
0.20 × 0.17 × 0.06 mm

Data collection

Bruker D8 VENTURE PHOTON 100 CMOS diffractometer
Radiation source: INCOATEC IμS micro–focus source
Mirror monochromator
Detector resolution: 10.4167 pixels mm^{-1}
ω scans
Absorption correction: multi-scan (*TWINABS*; Sheldrick, 2009)
T_{min} = 0.57, T_{max} = 0.84
12567 measured reflections
1895 independent reflections
1692 reflections with $I > 2\sigma(I)$
R_{int} = 0.040
θ_{max} = 72.4°, θ_{min} = 5.4°
h = −7→7
k = −17→17
l = −10→8

Refinement

Refinement on F^2
Least-squares matrix: full
$R[F^2 > 2\sigma(F^2)] = 0.042$
$wR(F^2) = 0.115$
$S = 1.07$
1895 reflections
147 parameters
0 restraints
Primary atom site location: structure-invariant direct methods
Secondary atom site location: difference Fourier map
Hydrogen site location: inferred from neighbouring sites
H-atom parameters constrained
$w = 1/[\sigma^2(F_o^2) + (0.0632P)^2 + 0.6053P]$ where $P = (F_o^2 + 2F_c^2)/3$
$(\Delta/\sigma)_{max} < 0.001$
$\Delta\rho_{max} = 0.31$ e Å^{-3}
$\Delta\rho_{min} = -0.33$ e Å^{-3}
Extinction correction: SHELXL2014/7 (Sheldrick, 2015b), $Fc^*=kFc[1+0.001xFc^2\lambda^3/\sin(2\theta)]^{-1/4}$
Extinction coefficient: 0.0045 (7)

Special details

Experimental. Analysis of 2191 reflections having I/σ(I) > 13 and chosen from the full data set with *CELL_NOW* (Sheldrick, 2008) showed the crystal to belong to the monoclinic system and to be twinned by a 180° rotation about the *c** axis. The raw data were processed using the multi-component version of *SAINT* under control of the two-component orientation file generated by *CELL_NOW*.

Geometry. All esds (except the esd in the dihedral angle between two l.s. planes) are estimated using the full covariance matrix. The cell esds are taken into account individually in the estimation of esds in distances, angles and torsion angles; correlations between esds in cell parameters are only used when they are defined by crystal symmetry. An approximate (isotropic) treatment of cell esds is used for estimating esds involving l.s. planes.

Refinement. Refinement of F^2 against ALL reflections. The weighted R-factor wR and goodness of fit S are based on F^2, conventional R-factors R are based on F, with F set to zero for negative F^2. The threshold expression of $F^2 > 2\text{sigma}(F^2)$ is used only for calculating R-factors(gt) etc. and is not relevant to the choice of reflections for refinement. R-factors based on F^2 are statistically about twice as large as those based on F, and R- factors based on ALL data will be even larger. H-atoms were placed in calculated positions (C—H = 0.95 - 0.98 Å) and included as riding contributions with isotropic displacement parameters 1.2 - 1.5 times those of the attached carbon atoms. Trial refinements with both the single-component data extracted with *TWINABS* and the full twinned data indicated that the former produced a more satisfactory model.

Fractional atomic coordinates and isotropic or equivalent isotropic displacement parameters (Å²)

	x	*y*	*z*	U_{iso}*/U_{eq}
N1	0.4176 (3)	0.86681 (11)	0.80398 (18)	0.0250 (4)
N2	−0.0598 (3)	0.77157 (13)	0.7824 (2)	0.0388 (5)
C1	0.3803 (4)	0.85654 (16)	0.9546 (2)	0.0349 (5)
H1A	0.2619	0.8911	0.9776	0.052*
H1B	0.5018	0.8752	1.0115	0.052*
H1C	0.3527	0.7966	0.9743	0.052*
C2	0.2757 (3)	0.83897 (13)	0.7044 (2)	0.0256 (4)
C3	0.3078 (4)	0.84670 (14)	0.5644 (2)	0.0308 (5)
H3	0.2084	0.8265	0.4957	0.037*
C4	0.4873 (4)	0.88441 (14)	0.5246 (2)	0.0341 (5)
H4	0.5129	0.8899	0.4282	0.041*
C5	0.6281 (4)	0.91379 (14)	0.6259 (3)	0.0350 (5)
H5	0.7506	0.9407	0.6000	0.042*
C6	0.5899 (3)	0.90390 (14)	0.7655 (2)	0.0311 (5)
H6	0.6876	0.9238	0.8355	0.037*
C7	0.0906 (3)	0.80090 (14)	0.7509 (2)	0.0286 (5)

P1	0.42105 (8)	0.58120 (3)	0.73007 (5)	0.0260 (2)
F1	0.3952 (3)	0.66725 (10)	0.81616 (18)	0.0499 (4)
F2	0.6643 (2)	0.59231 (10)	0.74158 (17)	0.0427 (4)
F3	0.4065 (2)	0.63247 (11)	0.58661 (16)	0.0499 (4)
F4	0.4482 (3)	0.49411 (10)	0.64785 (17)	0.0506 (4)
F5	0.4308 (2)	0.52981 (10)	0.87364 (15)	0.0471 (4)
F6	0.1770 (2)	0.56909 (11)	0.71904 (16)	0.0443 (4)

Atomic displacement parameters (Å²)

	U^{11}	U^{22}	U^{33}	U^{12}	U^{13}	U^{23}
N1	0.0252 (9)	0.0227 (9)	0.0271 (9)	0.0018 (7)	0.0011 (7)	−0.0016 (6)
N2	0.0349 (12)	0.0336 (11)	0.0478 (12)	−0.0043 (8)	0.0029 (9)	0.0027 (9)
C1	0.0381 (13)	0.0414 (13)	0.0248 (11)	0.0031 (10)	−0.0003 (9)	−0.0011 (9)
C2	0.0264 (11)	0.0195 (9)	0.0307 (10)	0.0033 (8)	−0.0006 (8)	0.0001 (8)
C3	0.0362 (12)	0.0249 (11)	0.0310 (11)	0.0002 (9)	−0.0023 (9)	0.0001 (8)
C4	0.0433 (14)	0.0273 (11)	0.0324 (12)	0.0021 (9)	0.0082 (10)	0.0018 (9)
C5	0.0323 (12)	0.0281 (11)	0.0453 (14)	−0.0012 (9)	0.0093 (10)	0.0001 (9)
C6	0.0273 (11)	0.0267 (11)	0.0391 (13)	−0.0001 (8)	0.0003 (9)	−0.0040 (9)
C7	0.0301 (12)	0.0250 (11)	0.0301 (10)	0.0003 (8)	−0.0033 (8)	0.0009 (8)
P1	0.0283 (3)	0.0249 (3)	0.0248 (3)	0.00132 (19)	0.0022 (2)	0.00086 (19)
F1	0.0546 (10)	0.0339 (8)	0.0603 (10)	0.0116 (7)	−0.0027 (7)	−0.0167 (7)
F2	0.0283 (8)	0.0477 (9)	0.0520 (9)	0.0000 (6)	0.0022 (6)	0.0001 (7)
F3	0.0482 (9)	0.0618 (10)	0.0400 (9)	0.0034 (7)	0.0036 (7)	0.0229 (7)
F4	0.0600 (10)	0.0387 (8)	0.0539 (9)	−0.0024 (7)	0.0104 (8)	−0.0192 (7)
F5	0.0528 (10)	0.0545 (9)	0.0347 (8)	0.0112 (7)	0.0074 (6)	0.0171 (7)
F6	0.0287 (8)	0.0613 (10)	0.0428 (8)	−0.0047 (6)	0.0017 (6)	0.0025 (7)

Geometric parameters (Å, º)

N1—C6	1.338 (3)	C4—C5	1.375 (4)
N1—C2	1.361 (3)	C4—H4	0.9500
N1—C1	1.482 (3)	C5—C6	1.380 (3)
N2—C7	1.141 (3)	C5—H5	0.9500
C1—H1A	0.9800	C6—H6	0.9500
C1—H1B	0.9800	P1—F3	1.5881 (14)
C1—H1C	0.9800	P1—F5	1.5899 (14)
C2—C3	1.371 (3)	P1—F4	1.5931 (15)
C2—C7	1.442 (3)	P1—F2	1.5953 (15)
C3—C4	1.386 (3)	P1—F1	1.5967 (15)
C3—H3	0.9500	P1—F6	1.6020 (15)
C6—N1—C2	119.82 (19)	C6—C5—H5	120.3
C6—N1—C1	120.14 (19)	N1—C6—C5	121.1 (2)
C2—N1—C1	120.04 (18)	N1—C6—H6	119.4
N1—C1—H1A	109.5	C5—C6—H6	119.4
N1—C1—H1B	109.5	N2—C7—C2	177.1 (2)
H1A—C1—H1B	109.5	F3—P1—F5	178.89 (9)

N1—C1—H1C	109.5	F3—P1—F4	90.74 (9)
H1A—C1—H1C	109.5	F5—P1—F4	89.38 (9)
H1B—C1—H1C	109.5	F3—P1—F2	90.76 (9)
N1—C2—C3	121.1 (2)	F5—P1—F2	90.35 (8)
N1—C2—C7	117.79 (19)	F4—P1—F2	89.37 (9)
C3—C2—C7	121.1 (2)	F3—P1—F1	90.70 (9)
C2—C3—C4	119.0 (2)	F5—P1—F1	89.19 (9)
C2—C3—H3	120.5	F4—P1—F1	178.54 (10)
C4—C3—H3	120.5	F2—P1—F1	90.37 (9)
C5—C4—C3	119.4 (2)	F3—P1—F6	89.67 (8)
C5—C4—H4	120.3	F5—P1—F6	89.23 (9)
C3—C4—H4	120.3	F4—P1—F6	90.24 (9)
C4—C5—C6	119.5 (2)	F2—P1—F6	179.43 (9)
C4—C5—H5	120.3	F1—P1—F6	90.00 (9)
C6—N1—C2—C3	1.3 (3)	C2—C3—C4—C5	−0.5 (3)
C1—N1—C2—C3	−179.1 (2)	C3—C4—C5—C6	1.1 (3)
C6—N1—C2—C7	−178.81 (19)	C2—N1—C6—C5	−0.7 (3)
C1—N1—C2—C7	0.8 (3)	C1—N1—C6—C5	179.7 (2)
N1—C2—C3—C4	−0.7 (3)	C4—C5—C6—N1	−0.5 (3)
C7—C2—C3—C4	179.4 (2)		

Hydrogen-bond geometry (Å, º)

D—H···*A*	*D*—H	H···*A*	*D*···*A*	*D*—H···*A*
C1—H1*A*···F4^{i}	0.98	2.40	3.161 (3)	134
C1—H1*B*···F6^{ii}	0.98	2.40	3.307 (3)	154
C4—H4···F6^{iii}	0.95	2.41	3.319 (3)	160
C5—H5···F5^{iv}	0.95	2.51	3.409 (3)	158

Symmetry codes: (i) −*x*+1/2, *y*+1/2, −*z*+3/2; (ii) *x*+1/2, −*y*+3/2, *z*+1/2; (iii) *x*+1/2, −*y*+3/2, *z*−1/2; (iv) −*x*+3/2, *y*+1/2, −*z*+3/2.

3-Cyano-1-methylpyridinium hexafluoridophosphate (2)

Crystal data

$C_7H_7N_2^+·PF_6^-$
M_r = 264.12
Orthorhombic, $P2_12_12_1$
a = 7.8484 (2) Å
b = 10.8964 (2) Å
c = 11.8669 (3) Å
V = 1014.85 (4) Å^3
Z = 4
F(000) = 528

D_x = 1.729 Mg m^{-3}
Cu *Kα* radiation, *λ* = 1.54178 Å
Cell parameters from 9953 reflections
θ = 3.7–72.4°
μ = 3.09 mm^{-1}
T = 150 K
Block, colourless
0.26 × 0.19 × 0.15 mm

Data collection

Bruker D8 VENTURE PHOTON 100 CMOS diffractometer
Radiation source: INCOATEC I*μ*S micro–focus source
Mirror monochromator

Detector resolution: 10.4167 pixels mm^{-1}
ω scans
Absorption correction: multi-scan (*SADABS*; Bruker, 2015)
T_{min} = 0.59, T_{max} = 0.65

15204 measured reflections
2009 independent reflections
1970 reflections with $I > 2\sigma(I)$
$R_{int} = 0.034$
$\theta_{max} = 72.3°$, $\theta_{min} = 5.5°$
$h = -9 \rightarrow 9$
$k = -13 \rightarrow 13$
$l = -14 \rightarrow 14$

Refinement

Refinement on F^2
Least-squares matrix: full
$R[F^2 > 2\sigma(F^2)] = 0.036$
$wR(F^2) = 0.095$
$S = 1.08$
2009 reflections
160 parameters
8 restraints
Primary atom site location: structure-invariant direct methods
Secondary atom site location: difference Fourier map
Hydrogen site location: inferred from neighbouring sites
H-atom parameters constrained
$w = 1/[\sigma^2(F_o^2) + (0.0513P)^2 + 0.5414P]$ where $P = (F_o^2 + 2F_c^2)/3$
$(\Delta/\sigma)_{max} < 0.001$
$\Delta\rho_{max} = 0.35$ e Å^{-3}
$\Delta\rho_{min} = -0.36$ e Å^{-3}
Extinction correction: *SHELXL* (Sheldrick, 2015b), $Fc^* = kFc[1+0.001xFc^2\lambda^3/\sin(2\theta)]^{-1/4}$
Extinction coefficient: 0.0095 (11)
Absolute structure: Flack *x* determined using 800 quotients $[(I^+)-(I^-)]/[(I^+)+(I^-)]$ (Parsons *et al.*, 2013)
Absolute structure parameter: 0.040 (6)

Special details

Geometry. All esds (except the esd in the dihedral angle between two l.s. planes) are estimated using the full covariance matrix. The cell esds are taken into account individually in the estimation of esds in distances, angles and torsion angles; correlations between esds in cell parameters are only used when they are defined by crystal symmetry. An approximate (isotropic) treatment of cell esds is used for estimating esds involving l.s. planes.

Refinement. Refinement of F^2 against ALL reflections. The weighted R-factor wR and goodness of fit S are based on F^2, conventional R-factors R are based on F, with F set to zero for negative F^2. The threshold expression of $F^2 > 2\text{sigma}(F^2)$ is used only for calculating R-factors(gt) etc. and is not relevant to the choice of reflections for refinement. R-factors based on F^2 are statistically about twice as large as those based on F, and R- factors based on ALL data will be even larger. H-atoms were placed in calculated positions (C—H = 0.95 - 0.98 Å) and included as riding contributions with isotropic displacement parameters 1.2 - 1.5 times those of the attached carbon atoms. The anion is rotationally disordered over two resolved sites about the F1···F4 axis in a 85/15 ratio. The disorder was refined with restraints that the two components have the same geometry.

Fractional atomic coordinates and isotropic or equivalent isotropic displacement parameters (Å²)

	x	*y*	*z*	U_{iso}*/U_{eq}	Occ. (<1)
N1	0.9719 (3)	0.3953 (2)	0.6993 (2)	0.0309 (5)	
N2	0.5379 (5)	0.3571 (3)	0.4213 (3)	0.0543 (8)	
C1	0.9963 (5)	0.3420 (3)	0.8133 (3)	0.0446 (8)	
H1A	1.0606	0.2652	0.8073	0.067*	
H1B	0.8849	0.3254	0.8475	0.067*	
H1C	1.0594	0.4001	0.8606	0.067*	
C2	0.8312 (4)	0.3669 (3)	0.6408 (3)	0.0316 (7)	
H2	0.7464	0.3157	0.6733	0.038*	
C3	0.8100 (4)	0.4122 (3)	0.5329 (3)	0.0318 (7)	
C4	0.9332 (4)	0.4882 (3)	0.4868 (3)	0.0376 (7)	
H4	0.9196	0.5206	0.4131	0.045*	
C5	1.0763 (5)	0.5159 (4)	0.5499 (3)	0.0429 (8)	
H5	1.1621	0.5680	0.5198	0.051*	
C6	1.0937 (4)	0.4676 (3)	0.6563 (3)	0.0370 (7)	

H6	1.1924	0.4856	0.6995	0.044*	
C7	0.6579 (5)	0.3806 (3)	0.4718 (3)	0.0396 (8)	
P1	0.53561 (10)	0.67446 (7)	0.67835 (6)	0.0304 (2)	
F1	0.6869 (4)	0.6015 (3)	0.7338 (2)	0.0688 (8)	
F4	0.3803 (3)	0.7456 (3)	0.6233 (3)	0.0786 (9)	
F2	0.6590 (4)	0.7059 (3)	0.5769 (2)	0.0553 (8)	0.848 (3)
F3	0.4755 (4)	0.5537 (3)	0.6115 (3)	0.0647 (9)	0.848 (3)
F5	0.5888 (5)	0.7938 (3)	0.7430 (4)	0.0835 (14)	0.848 (3)
F6	0.4049 (4)	0.6385 (2)	0.7769 (2)	0.0522 (8)	0.848 (3)
F2A	0.599 (2)	0.664 (2)	0.5531 (6)	0.0553 (8)	0.152 (3)
F3A	0.481 (2)	0.5344 (7)	0.6895 (17)	0.0647 (9)	0.152 (3)
F5A	0.606 (2)	0.8092 (8)	0.679 (2)	0.0835 (14)	0.152 (3)
F6A	0.4950 (19)	0.6976 (14)	0.8095 (6)	0.0522 (8)	0.152 (3)

Atomic displacement parameters (Å²)

	U^{11}	U^{22}	U^{33}	U^{12}	U^{13}	U^{23}
N1	0.0269 (11)	0.0281 (12)	0.0378 (13)	0.0013 (11)	0.0057 (11)	0.0006 (10)
N2	0.0478 (18)	0.0555 (19)	0.0597 (19)	−0.0142 (16)	−0.0071 (18)	−0.0133 (16)
C1	0.0425 (19)	0.0486 (19)	0.0428 (17)	−0.0023 (15)	−0.0016 (15)	0.0112 (15)
C2	0.0278 (15)	0.0254 (13)	0.0416 (16)	−0.0037 (12)	0.0070 (12)	−0.0030 (11)
C3	0.0314 (15)	0.0234 (13)	0.0406 (16)	−0.0029 (12)	0.0030 (13)	−0.0071 (12)
C4	0.0423 (19)	0.0321 (15)	0.0385 (16)	−0.0098 (14)	0.0023 (14)	−0.0003 (13)
C5	0.0374 (18)	0.0435 (19)	0.0477 (19)	−0.0147 (15)	0.0036 (15)	0.0047 (15)
C6	0.0286 (15)	0.0370 (17)	0.0453 (18)	−0.0060 (13)	0.0026 (13)	0.0000 (14)
C7	0.0397 (17)	0.0359 (16)	0.0431 (17)	−0.0079 (14)	−0.0002 (15)	−0.0096 (15)
P1	0.0261 (4)	0.0322 (4)	0.0331 (4)	0.0031 (3)	0.0033 (3)	0.0003 (3)
F1	0.0616 (15)	0.095 (2)	0.0500 (13)	0.0445 (15)	−0.0073 (12)	0.0000 (13)
F4	0.0455 (14)	0.090 (2)	0.100 (2)	0.0266 (14)	−0.0090 (14)	0.0258 (19)
F2	0.0416 (16)	0.078 (2)	0.0465 (14)	−0.0058 (14)	0.0129 (13)	0.0148 (14)
F3	0.0441 (13)	0.0667 (17)	0.083 (2)	−0.0172 (14)	0.0128 (17)	−0.0386 (17)
F5	0.0592 (17)	0.0662 (19)	0.125 (4)	−0.0103 (14)	0.011 (2)	−0.064 (2)
F6	0.0469 (15)	0.0530 (16)	0.0567 (15)	0.0087 (11)	0.0262 (13)	0.0062 (12)
F2A	0.0416 (16)	0.078 (2)	0.0465 (14)	−0.0058 (14)	0.0129 (13)	0.0148 (14)
F3A	0.0441 (13)	0.0667 (17)	0.083 (2)	−0.0172 (14)	0.0128 (17)	−0.0386 (17)
F5A	0.0592 (17)	0.0662 (19)	0.125 (4)	−0.0103 (14)	0.011 (2)	−0.064 (2)
F6A	0.0469 (15)	0.0530 (16)	0.0567 (15)	0.0087 (11)	0.0262 (13)	0.0062 (12)

Geometric parameters (Å, º)

N1—C6	1.340 (4)	C5—C6	1.375 (5)
N1—C2	1.341 (4)	C5—H5	0.9500
N1—C1	1.485 (4)	C6—H6	0.9500
N2—C7	1.145 (5)	P1—F5	1.567 (3)
C1—H1A	0.9800	P1—F5A	1.569 (6)
C1—H1B	0.9800	P1—F2A	1.572 (6)
C1—H1C	0.9800	P1—F1	1.573 (2)
C2—C3	1.382 (5)	P1—F2	1.582 (2)

C2—H2	0.9500	P1—F4	1.586 (3)
C3—C4	1.385 (4)	P1—F3A	1.590 (6)
C3—C7	1.438 (5)	P1—F6	1.604 (2)
C4—C5	1.383 (5)	P1—F3	1.607 (3)
C4—H4	0.9500	P1—F6A	1.608 (6)
C6—N1—C2	121.7 (3)	F5A—P1—F1	101.8 (8)
C6—N1—C1	119.1 (3)	F2A—P1—F1	96.9 (7)
C2—N1—C1	119.2 (3)	F5—P1—F2	91.7 (2)
N1—C1—H1A	109.5	F1—P1—F2	88.03 (15)
N1—C1—H1B	109.5	F5—P1—F4	90.1 (2)
H1A—C1—H1B	109.5	F5A—P1—F4	79.4 (8)
N1—C1—H1C	109.5	F2A—P1—F4	83.6 (7)
H1A—C1—H1C	109.5	F1—P1—F4	178.71 (18)
H1B—C1—H1C	109.5	F2—P1—F4	92.93 (16)
N1—C2—C3	119.8 (3)	F5A—P1—F3A	172.8 (10)
N1—C2—H2	120.1	F2A—P1—F3A	95.4 (10)
C3—C2—H2	120.1	F1—P1—F3A	71.5 (7)
C2—C3—C4	119.7 (3)	F4—P1—F3A	107.3 (7)
C2—C3—C7	118.8 (3)	F5—P1—F6	90.9 (2)
C4—C3—C7	121.6 (3)	F1—P1—F6	93.12 (15)
C5—C4—C3	119.0 (3)	F2—P1—F6	177.11 (18)
C5—C4—H4	120.5	F4—P1—F6	85.88 (16)
C3—C4—H4	120.5	F5—P1—F3	178.3 (2)
C6—C5—C4	119.5 (3)	F1—P1—F3	90.83 (19)
C6—C5—H5	120.2	F2—P1—F3	88.94 (18)
C4—C5—H5	120.2	F4—P1—F3	88.3 (2)
N1—C6—C5	120.3 (3)	F6—P1—F3	88.39 (17)
N1—C6—H6	119.8	F5A—P1—F6A	85.2 (11)
C5—C6—H6	119.8	F2A—P1—F6A	171.6 (9)
N2—C7—C3	178.5 (4)	F1—P1—F6A	79.9 (5)
F5A—P1—F2A	87.9 (12)	F4—P1—F6A	99.8 (5)
F5—P1—F1	90.8 (2)	F3A—P1—F6A	91.0 (9)
C6—N1—C2—C3	0.3 (4)	C7—C3—C4—C5	179.6 (3)
C1—N1—C2—C3	−177.6 (3)	C3—C4—C5—C6	0.2 (5)
N1—C2—C3—C4	−0.9 (4)	C2—N1—C6—C5	0.5 (5)
N1—C2—C3—C7	−179.9 (3)	C1—N1—C6—C5	178.5 (3)
C2—C3—C4—C5	0.7 (5)	C4—C5—C6—N1	−0.8 (6)

Hydrogen-bond geometry (Å, º)

D—H···*A*	*D*—H	H···*A*	*D*···*A*	*D*—H···*A*
C1—H1*B*···F4^{i}	0.98	2.28	3.225 (5)	161
C2—H2···F6^{i}	0.95	2.34	3.253 (4)	160
C6—H6···F6^{ii}	0.95	2.53	3.389 (5)	150

Symmetry codes: (i) −*x*+1, *y*−1/2, −*z*+3/2; (ii) *x*+1, *y*, *z*.

4-Cyano-1-methylpyridinium hexafluoridophosphate (3)

Crystal data

$C_7H_7N_2^+ \cdot PF_6^-$
$M_r = 264.12$
Orthorhombic, $P2_12_12_1$
$a = 8.5293$ (6) Å
$b = 8.6264$ (7) Å
$c = 13.3589$ (10) Å
$V = 982.91$ (13) Å^3
$Z = 4$
$F(000) = 528$
$D_x = 1.785$ Mg m^{-3}
Mo $K\alpha$ radiation, $\lambda = 0.71073$ Å
Cell parameters from 9502 reflections
$\theta = 2.8$–$29.1°$
$\mu = 0.34$ mm^{-1}
$T = 150$ K
Block, colourless
0.26 × 0.19 × 0.13 mm

Data collection

Bruker SMART APEX CCD diffractometer
Radiation source: fine-focus sealed tube
Graphite monochromator
Detector resolution: 8.3333 pixels mm^{-1}
φ and ω scans
Absorption correction: multi-scan (*SADABS*; Bruker, 2015)
$T_{min} = 0.89$, $T_{max} = 0.96$
19081 measured reflections
2642 independent reflections
2420 reflections with $I > 2\sigma(I)$
$R_{int} = 0.033$
$\theta_{max} = 29.2°$, $\theta_{min} = 2.8°$
$h = -11 \rightarrow 11$
$k = -11 \rightarrow 11$
$l = -18 \rightarrow 18$

Refinement

Refinement on F^2
Least-squares matrix: full
$R[F^2 > 2\sigma(F^2)] = 0.031$
$wR(F^2) = 0.084$
$S = 1.13$
2642 reflections
146 parameters
0 restraints
Primary atom site location: structure-invariant direct methods
Secondary atom site location: difference Fourier map
Hydrogen site location: inferred from neighbouring sites
H-atom parameters constrained
$w = 1/[\sigma^2(F_o^2) + (0.0536P)^2 + 0.0393P]$ where $P = (F_o^2 + 2F_c^2)/3$
$(\Delta/\sigma)_{max} = 0.006$
$\Delta\rho_{max} = 0.31$ e Å^{-3}
$\Delta\rho_{min} = -0.20$ e Å^{-3}
Absolute structure: Flack *x* determined using 988 quotients $[(I^+)-(I^-)]/[(I^+)+(I^-)]$ (Parsons *et al.*, 2013)
Absolute structure parameter: −0.01 (3)

Special details

Experimental. The diffraction data were obtained from 3 sets of 400 frames, each of width 0.5° in ω, colllected at φ = 0.00, 90.00 and 180.00° and 2 sets of 800 frames, each of width 0.45° in φ, collected at ω = –30.00 and 210.00°. The scan time was 15 sec/frame.

Geometry. All esds (except the esd in the dihedral angle between two l.s. planes) are estimated using the full covariance matrix. The cell esds are taken into account individually in the estimation of esds in distances, angles and torsion angles; correlations between esds in cell parameters are only used when they are defined by crystal symmetry. An approximate (isotropic) treatment of cell esds is used for estimating esds involving l.s. planes.

Refinement. Refinement of F^2 against ALL reflections. The weighted R-factor wR and goodness of fit S are based on F^2, conventional R-factors R are based on F, with F set to zero for negative F^2. The threshold expression of $F^2 > 2$sigma(F^2) is used only for calculating R-factors(gt) etc. and is not relevant to the choice of reflections for refinement. R-factors based on F^2 are statistically about twice as large as those based on F, and R- factors based on ALL data will be even larger. H-atoms attached to carbon were placed in calculated positions (C—H = 0.95 - 0.98 Å). All were included as riding contributions with isotropic displacement parameters 1.2 - 1.5 times those of the attached atoms.

Fractional atomic coordinates and isotropic or equivalent isotropic displacement parameters (Å²)

	x	*y*	*z*	U_{iso}*/U_{eq}
N1	0.3277 (2)	0.58167 (17)	0.44131 (12)	0.0197 (3)
N2	0.5725 (2)	0.0199 (2)	0.39214 (14)	0.0317 (4)
C1	0.2618 (3)	0.7396 (2)	0.45537 (17)	0.0280 (5)
H1A	0.3475	0.8152	0.4583	0.042*
H1B	0.2020	0.7431	0.5179	0.042*
H1C	0.1925	0.7647	0.3991	0.042*
C2	0.4065 (2)	0.5148 (3)	0.51769 (14)	0.0226 (4)
H2	0.4191	0.5693	0.5790	0.027*
C3	0.4688 (2)	0.3685 (2)	0.50746 (15)	0.0231 (4)
H3	0.5244	0.3211	0.5609	0.028*
C4	0.4481 (2)	0.2915 (2)	0.41667 (15)	0.0204 (4)
C5	0.3665 (2)	0.3617 (2)	0.33903 (15)	0.0230 (4)
H5	0.3519	0.3096	0.2771	0.028*
C6	0.3075 (2)	0.5081 (2)	0.35368 (14)	0.0222 (4)
H6	0.2517	0.5579	0.3012	0.027*
C7	0.5161 (3)	0.1389 (2)	0.40273 (16)	0.0246 (4)
P1	0.32732 (6)	0.01238 (6)	0.69107 (4)	0.02273 (14)
F1	0.22985 (17)	0.16304 (16)	0.72363 (11)	0.0386 (4)
F2	0.48612 (19)	0.1071 (2)	0.70429 (16)	0.0594 (5)
F3	0.3350 (2)	−0.04134 (17)	0.80554 (10)	0.0471 (4)
F4	0.42360 (18)	−0.13840 (19)	0.65850 (12)	0.0446 (4)
F5	0.16725 (16)	−0.08286 (15)	0.67718 (10)	0.0326 (3)
F6	0.31409 (19)	0.06562 (16)	0.57645 (10)	0.0403 (4)

Atomic displacement parameters (Å²)

	U^{11}	U^{22}	U^{33}	U^{12}	U^{13}	U^{23}
N1	0.0209 (7)	0.0168 (7)	0.0213 (8)	−0.0018 (7)	0.0018 (6)	0.0005 (6)
N2	0.0355 (10)	0.0287 (9)	0.0310 (10)	0.0060 (8)	−0.0003 (8)	0.0012 (8)
C1	0.0374 (12)	0.0178 (9)	0.0289 (12)	0.0031 (8)	0.0009 (9)	−0.0037 (8)
C2	0.0259 (9)	0.0248 (9)	0.0171 (8)	−0.0056 (8)	−0.0023 (7)	−0.0018 (8)
C3	0.0238 (9)	0.0243 (10)	0.0213 (10)	−0.0036 (8)	−0.0035 (7)	0.0035 (8)
C4	0.0186 (8)	0.0195 (8)	0.0229 (9)	−0.0027 (7)	0.0013 (7)	0.0010 (7)
C5	0.0280 (10)	0.0218 (9)	0.0192 (9)	−0.0021 (7)	−0.0015 (7)	−0.0023 (7)
C6	0.0255 (9)	0.0215 (8)	0.0195 (9)	−0.0004 (8)	−0.0031 (7)	0.0018 (7)
C7	0.0257 (10)	0.0261 (10)	0.0220 (10)	0.0001 (8)	−0.0008 (8)	0.0017 (8)
P1	0.0237 (2)	0.0204 (2)	0.0241 (3)	0.00204 (19)	−0.00338 (19)	−0.00227 (19)
F1	0.0487 (8)	0.0299 (7)	0.0372 (8)	0.0158 (6)	−0.0114 (7)	−0.0105 (6)
F2	0.0318 (7)	0.0491 (9)	0.0972 (15)	−0.0113 (7)	−0.0132 (10)	−0.0124 (10)
F3	0.0709 (10)	0.0456 (8)	0.0246 (7)	0.0168 (8)	−0.0175 (7)	0.0008 (6)
F4	0.0438 (8)	0.0377 (8)	0.0524 (10)	0.0207 (7)	−0.0057 (7)	−0.0131 (7)
F5	0.0298 (6)	0.0325 (6)	0.0357 (7)	−0.0074 (6)	−0.0027 (6)	0.0051 (6)
F6	0.0550 (10)	0.0379 (7)	0.0281 (7)	−0.0040 (7)	0.0091 (7)	0.0076 (6)

Geometric parameters (Å, º)

N1—C6	1.343 (2)	C4—C5	1.388 (3)
N1—C2	1.351 (2)	C4—C7	1.451 (3)
N1—C1	1.486 (2)	C5—C6	1.374 (3)
N2—C7	1.142 (3)	C5—H5	0.9500
C1—H1A	0.9800	C6—H6	0.9500
C1—H1B	0.9800	P1—F2	1.5918 (16)
C1—H1C	0.9800	P1—F4	1.5985 (14)
C2—C3	1.376 (3)	P1—F3	1.5992 (15)
C2—H2	0.9500	P1—F6	1.6026 (15)
C3—C4	1.394 (3)	P1—F1	1.6030 (14)
C3—H3	0.9500	P1—F5	1.6042 (14)
C6—N1—C2	121.37 (17)	C4—C5—H5	120.7
C6—N1—C1	119.67 (17)	N1—C6—C5	120.78 (18)
C2—N1—C1	118.95 (17)	N1—C6—H6	119.6
N1—C1—H1A	109.5	C5—C6—H6	119.6
N1—C1—H1B	109.5	N2—C7—C4	178.6 (2)
H1A—C1—H1B	109.5	F2—P1—F4	90.63 (9)
N1—C1—H1C	109.5	F2—P1—F3	90.45 (10)
H1A—C1—H1C	109.5	F4—P1—F3	90.20 (8)
H1B—C1—H1C	109.5	F2—P1—F6	91.08 (10)
N1—C2—C3	120.56 (19)	F4—P1—F6	90.54 (9)
N1—C2—H2	119.7	F3—P1—F6	178.30 (10)
C3—C2—H2	119.7	F2—P1—F1	89.70 (9)
C2—C3—C4	118.32 (19)	F4—P1—F1	179.67 (9)
C2—C3—H3	120.8	F3—P1—F1	89.81 (9)
C4—C3—H3	120.8	F6—P1—F1	89.45 (8)
C5—C4—C3	120.40 (19)	F2—P1—F5	179.72 (10)
C5—C4—C7	120.02 (19)	F4—P1—F5	89.37 (9)
C3—C4—C7	119.56 (19)	F3—P1—F5	89.83 (8)
C6—C5—C4	118.57 (19)	F6—P1—F5	88.64 (8)
C6—C5—H5	120.7	F1—P1—F5	90.30 (8)
C6—N1—C2—C3	0.1 (3)	C3—C4—C5—C6	0.2 (3)
C1—N1—C2—C3	179.82 (18)	C7—C4—C5—C6	−178.13 (17)
N1—C2—C3—C4	−0.1 (3)	C2—N1—C6—C5	0.1 (3)
C2—C3—C4—C5	0.0 (3)	C1—N1—C6—C5	−179.63 (18)
C2—C3—C4—C7	178.32 (18)	C4—C5—C6—N1	−0.2 (3)

Hydrogen-bond geometry (Å, º)

D—H···*A*	*D*—H	H···*A*	*D*···*A*	*D*—H···*A*
C5—H5···F5^{i}	0.95	2.37	3.247 (2)	153

C3—H3···F3^{ii}	0.95	2.46	3.106 (2)	126
C1—H1*C*···F1^{iii}	0.98	2.51	3.208 (3)	128

Symmetry codes: (i) −*x*+1/2, −*y*, *z*−1/2; (ii) −*x*+1, *y*+1/2, −*z*+3/2; (iii) −*x*+1/2, −*y*+1, *z*−1/2.